

Multi-material topology optimization of Reissner-Mindlin plates using MITC4

Thien Thanh Banh^a and Dongkyu Lee^{*}

Department of Architectural Engineering, Sejong University, Seoul 05006, Republic of Korea

(Received April 6, 2017, Revised January 16, 2018, Accepted January 24, 2018)

Abstract. In this study, a mixed-interpolated tensorial component 4 nodes method (MITC4) is treated as a numerical analysis model for topology optimization using multiple materials assigned within Reissner-Mindlin plates. Multi-material optimal topology and shape are produced as alternative plate retrofit designs to provide reasonable material assignments based on stress distributions. Element density distribution contours of mixing multiple material densities are linked to Solid Isotropic Material with Penalization (SIMP) as a design model. Mathematical formulation of multi-material topology optimization problem solving minimum compliance is an alternating active-phase algorithm with the Gauss-Seidel version as an optimization model of optimality criteria. Numerical examples illustrate the reliability and accuracy of the present design method for multi-material topology optimization with Reissner-Mindlin plates using MITC4 elements and steel materials.

Keywords: multi-materials topology optimization; MITC4; Reissner-Mindlin theory; finite element method; steel plate; shearlocking

1. Introduction

In recent years, computer-aided topology optimization has been in increasing attention. Since the pioneering study by Bendtsøe and Kikuchi (1988), structural optimization has made a remarkable progress as an innovative numerical and design method, attracting enormous amounts of attention from scientific communities (e.g., Lee *et al.* 2012, 2016a Lee and Shin 2015a, b, 2016a, Doan and Lee 2017, Banh and Lee 2018). In the field of topology optimization, multi-material topology optimization finds the optimal density distribution of different types of material in given conditions. Zhou and Wang (2006) introduced a phase field method for the multi-material structural topology optimization with a generalized Cahn-Hilliard model. Sigmund and Torquato (1997) introduced the design of materials with extreme thermal expansion using the three-phase topology optimization method. Alonso *et al.* (2014) studied topology synthesis of multiple materials by using a multi Sequential Element Rejection and Admission (SERA) method. Yun and Youn (2017) investigated optimized topologies using multiple materials for viscoelastically damped structures under time-dependent loading. Composite materials are generally made of two or more constituent multi-materials with variant mechanical properties and have advantageous overall characteristics. When compared to traditional material, Xia *et al.* (2018) proposed a numerical framework for optimizing the fracture resistance of quasi-brittle composites through a modification of the topology of the inclusion phase.

Regarding the numerical simulation of optimized topology problems for plate structures, by using Reissner-Mindlin plate theory, Belblidia *et al.* (2001) presented a novel topology optimization algorithm for single- or three-layered artificial material model. Goo *et al.* (2016) studied optimal topologies for thin plate structures with bending stress constraints. Yan *et al.* (2016) studied optimal topology design of damped vibrating plate structures subject to initial excitations. Nevertheless, adding hard materials with the same amount of total material may produce stiffer structures than single material.

The Reissner-Mindlin theory of plates is an extension of Kirchhoff-Love plate theory that takes into account shear deformations through the thickness of a plate. Therefore Reissner-Mindlin plate bending model has a wider range of applicability than the Kirchhoff-Love model (Arnold *et al.* 2002). This study focuses on the application of multiple materials to topology optimization of plate structures by using Reissner-Mindlin plate theory. To overcome shear locking phenomenon of thick plate, a MITC (mixed interpolation of tensorial components) (Bathe and Dvorkin 1985) approach is used, instead of a classical reduced integration. This element interpolates the out-of-plane shear stresses using collocation points at the element boundaries. It uses the standard bending stiffness part, and the shear stiffness part is replaced by the mixed interpolation of tensorial components. To discover the multi-material design distribution in structure, the alternating active phase algorithm of optimal criteria introduced by Tavakoli and Mohseni (2014) is used. The multi-material-phase field approach is based on the Cahn-Hilliard equation, and a general method to solve multiphase structure topology optimization problems was presented in Zhou and Wang (2006). Due to simplicity and efficiency in topology optimization problem with single constraint and objective

*Corresponding author, Associate Professor,
E-mail: dongkyulee@sejong.ac.kr

^a Ph.D. Student

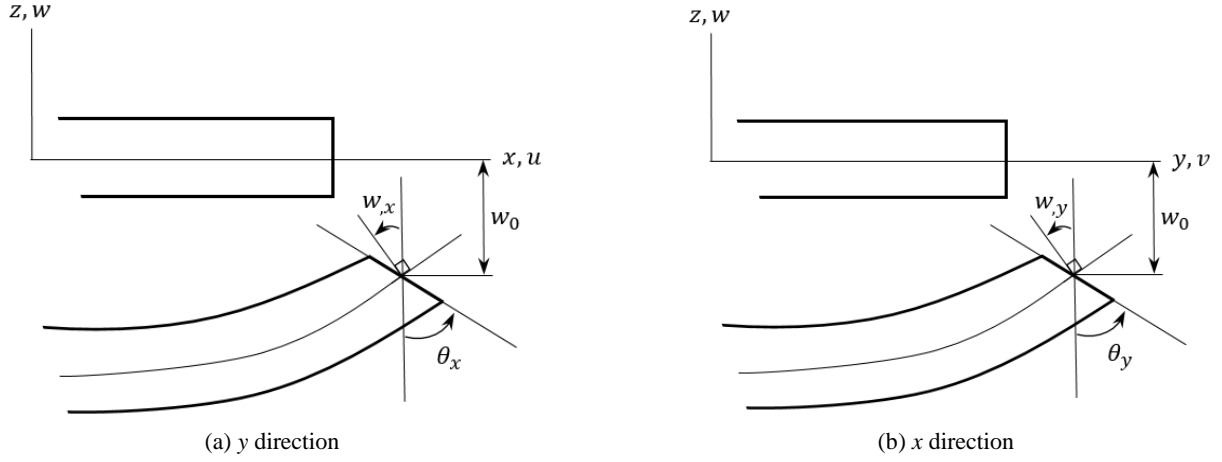


Fig. 1 Deformed plate cross section view in two directions

function, Optimality Criteria method (Andreassen *et al.* 2011) is used in this study.

The obtained numerical example results demonstrate the success, performance, and effectiveness of the present method. This study contributes to give engineers and designers design information for plate-like structures by using multi-material topology optimization.

The body of this study begins in Section 2 with a brief of Reissner–Mindlin plate theory. In Section 3, an analysis model of multi-material topology problem as well as stiffness formulation and sensitivity analysis of compliance for plates structures are described, including the computation procedure of multi-material topology optimization of Reissner–Mindlin for plate structures. Section 4 shows numerical applications to verify the present method. Conclusions and remark are presented in Section 5.

2. Finite element formulation of MITC4 for Mindlin plates

2.1 A brief of Reissner–Mindlin plate theory

Reissner–Mindlin plate model determines functions w and (θ_x, θ_y) as shown in Fig. 1, which are defined as transverse displacement and the rotation vectors, respectively, in the middle surface of the plate. Total plate energy Π based on potential energy for bending and shear is written as

$$\Pi = \frac{1}{2} \int_{\Omega} \boldsymbol{\kappa}^T \mathbf{D}_b \boldsymbol{\kappa} + \frac{1}{2} \int_{\Omega} \boldsymbol{\gamma}^T \mathbf{D}_s \boldsymbol{\gamma} - \Pi_{ext} \quad (1)$$

with Π_{ext} is the potential energy of the applied loads and

$$\boldsymbol{\kappa} = [\theta_{x,x} \quad \theta_{y,y} \quad \theta_{x,y} + \theta_{y,x}]^T; \quad \boldsymbol{\gamma} = [w_{,x} + \theta_x \quad w_{,y} + \theta_y]^T \quad (2)$$

where

$$\mathbf{D}_b = \frac{Et^3}{12(1-\nu^2)} \begin{bmatrix} 1 & \nu & 0 \\ \nu & 1 & 0 \\ 0 & 0 & (1-\nu)/2 \end{bmatrix}; \quad \mathbf{D}_s = Gt\kappa \begin{bmatrix} 1 & 0 \\ 0 & 1 \end{bmatrix} \quad (3)$$

where $G = E / 2(1+\nu)$, t is thickness. E is Young's modulus and ν is Poisson's ratio. Shear correction factor κ is chosen to be $5/6$ for the purpose of removal of shear locking.

2.2 Finite element implementation (Q4)

In finite element method, the sectional rotations and the transverse mid-surface displacements are bilinearly interpolated as

$$\theta_x = \sum_{i=1}^4 N_i^e \theta_{xi}; \quad \theta_y = \sum_{i=1}^4 N_i^e \theta_{yi}; \quad w = \sum_{i=1}^4 N_i^e w_i \quad (4)$$

where θ_{xi} , θ_{yi} , and w_i are the nodal point values of the variables θ_x , θ_y , and w , respectively. The curvature-displacement and shear strain-displacement relations are written as

$$\boldsymbol{\kappa} = \sum_{i=1}^4 \mathbf{B}_{bi} \mathbf{q}_i; \quad \boldsymbol{\gamma} = \sum_{i=1}^4 \mathbf{B}_{si} \mathbf{q}_i \quad (5)$$

where $\mathbf{q}_i = [w_i \quad \theta_{xi} \quad \theta_{yi}]^T$ is an unknown value at node i . The curvature-displacement matrix and strain-displacement matrix are written as

$$\mathbf{B}_{bi} = \begin{bmatrix} 0 & N_{i,x}^e & 0 \\ 0 & 0 & N_{i,y}^e \\ 0 & N_{i,y}^e & N_{i,x}^e \end{bmatrix}; \quad \mathbf{B}_{si} = \begin{bmatrix} N_{i,x}^e & N_i^e & 0 \\ N_{i,y}^e & 0 & N_i^e \end{bmatrix} \quad (6)$$

2.3 Mixed-interpolated tensorial components 4 nodes element

According to Reissner–Mindlin plate theory, the deflection and the rotation are independently defined each other. In bilinear interpolation for displacements and rotations, transverse shear strains appear at all points in the element subjected to a constant bending moment. Therefore, the low-order standard iso-parametric displacement-based plate elements without special treatments produce poor results in the thin plate case due to the false shear strains which result in the shear locking

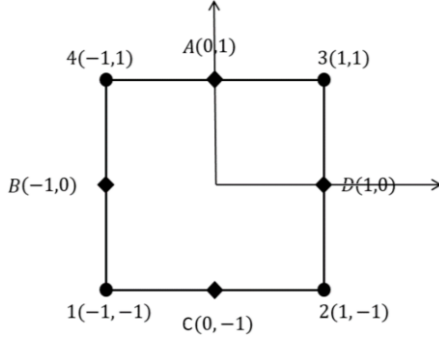


Fig. 2 MITC4 element

phenomenon. In the classical approach to avoid this deficiency, the shear part of the stiffness matrix is integrated by using 1×1 Gauss quadrature. In the present work, MITC (mixed interpolation of tensorial components) by Bathe and Dvorkin (1985) approach is utilized to eliminate shear locking.

In MITC4, the bending stiffness part is approximated as above section, and the approximation of the shear strains components may be expressed as

$$\begin{aligned}\gamma_x &= N_1^s \gamma_{xz}^B + N_2^s \gamma_{xz}^D \\ \gamma_y &= N_3^s \gamma_{yz}^A + N_4^s \gamma_{yz}^C\end{aligned}\quad (7)$$

where the components of $\{N_k^s\}_{k=1:4}$ and $\gamma_{xz}^A, \gamma_{xz}^B, \gamma_{yz}^C, \gamma_{yz}^D$ are shown as follows.

$$\begin{aligned}N_1^s &= \frac{1}{2}(1-\eta), & N_2^s &= \frac{1}{2}(1+\eta), \\ N_3^s &= \frac{1}{2}(1-\xi), & N_4^s &= \frac{1}{2}(1+\xi),\end{aligned}\quad (8)$$

and

$$\begin{aligned}\gamma_{xz}^A &= -\frac{w_3 - w_4}{a} + \frac{\beta_{x3} + \beta_{x4}}{2}, & \gamma_{xz}^C &= -\frac{w_2 - w_1}{a} + \frac{\beta_{x1} + \beta_{x2}}{2} \\ \gamma_{yx}^D &= -\frac{w_3 - w_2}{b} + \frac{\beta_{y3} + \beta_{y2}}{2}, & \gamma_{yz}^B &= -\frac{w_4 - w_1}{b} + \frac{\beta_{y1} + \beta_{y4}}{2}\end{aligned}\quad (9)$$

where a and b are respectively the lengths of edges connected by vertices 1-2 and 1-4. The approximation of the shear strains may be re-written as follows.

$$\boldsymbol{\gamma}^s = \begin{Bmatrix} \gamma_x \\ \gamma_y \end{Bmatrix} = \begin{bmatrix} N_1^s & N_2^s & 0 & 0 \\ 0 & 0 & N_3^s & N_4^s \end{bmatrix} \begin{Bmatrix} \gamma_{xz}^C \\ \gamma_{xz}^A \\ \gamma_{yz}^B \\ \gamma_{yz}^D \end{Bmatrix} = \mathbf{B}_s \mathbf{q} \quad (10)$$

where the shear part of the shear stiffness matrix is written as follows.

$$\mathbf{B}_s = \begin{bmatrix} \frac{N_1^s}{a} & \frac{N_1^s}{2} & 0 & -\frac{N_1^s}{a} & \frac{N_1^s}{2} & 0 & -\frac{N_2^s}{a} & \frac{N_2^s}{2} & 0 & \frac{N_2^s}{a} & \frac{N_2^s}{2} & 0 \\ \frac{N_3^s}{b} & 0 & \frac{N_3^s}{2} & \frac{N_4^s}{b} & 0 & \frac{N_4^s}{2} & -\frac{N_4^s}{b} & 0 & \frac{N_4^s}{2} & -\frac{N_3^s}{b} & 0 & \frac{N_3^s}{2} \end{bmatrix} \quad (11)$$

3. Topology optimization formulation for multiple materials

3.1 Multi-phase topology optimization

Similar to topology optimization for single material, multi-material topology optimization is an optimization technique that seeks an optimal layout in a given design domain by using multiple materials. It typically uses finite element method (FEM) and sensitivity analysis as an analysis model. In topology optimization, the minimum structural compliance is often sought, with relative densities as the only design parameters. Element densities are set as design variables which can physically attain integer values, i.e., $\alpha_i \in \{0, 1\}$. A single element may contain multiple material densities corresponding to a number of contributed materials. To avoid singularities in computation, material densities are relaxed for densities between 0 and 1 by a very small lower bound non-zero value ε_i . The general mathematical formulation of problem is written as follows.

$$\begin{aligned}\text{minimize: } & C(\boldsymbol{\alpha}, \mathbf{U}) = \mathbf{U}^T \mathbf{K} \mathbf{U} \\ \text{subject to: } & \mathbf{K}(\boldsymbol{\alpha}) \mathbf{U} = \mathbf{F} \\ & \int_{\Omega} \alpha_i dx \leq V_i \\ & 0 < \varepsilon_i \leq \alpha_i \leq 1\end{aligned}\quad (12)$$

where C is structural compliance. α_i is the density vector for phase material i -th. V_i is the per-material volume fraction constraint with $i = 1 : n + 1$ such that the summation should be equal to unity $\sum_i V_i = 1$. \mathbf{U} and \mathbf{F} are global load and displacement vectors, respectively. \mathbf{K} is global stiffness matrix and Ω is a given design domain.

3.2 Alternating active-phase algorithm

Through alternating active phase algorithm, the multi-phase topology optimization problem is solved by converting multi-phase into $p(p-1)/2$ binary phases sub-problem. Each binary sub-problem is a so-called active phase. The binary phase material densities α_j are modified to α_{ab} , with 'a' and 'b' which denote the active phase. Overlaps are not allowed in a desired optimal design, and then summation of the densities at each point $x \in \Omega$ should be equal to unity $\sum_{j=1}^p \alpha_j = 1$. The densities summation of two active phases 'a' and 'b' at each location x for each sub-problem may be calculated as follows

$$\alpha_a(x) + \alpha_b(x) = 1 - \sum_{i=1, i \neq \{a,b\}}^{n+1} \alpha_i(x) \quad (13)$$

Therefore, the summation of per-material volume fraction constraints V_i should be equal to unity as follows.

$$\sum_{i=1}^p V_i(x) = 1 \quad (14)$$

3.3 Compliance sensitivity formulation for stiffness of Reissner-Mindlin plate in terms of multi-material densities

The stiffness matrix is given as follows.

$$\mathbf{K}^e = \sum_{r=\{b,s\}} \mathbf{K}_r^e = \sum_{r=\{b,s\}} \int_{\Omega^e} \mathbf{B}_r^T \left(\sum_{k=1}^{n+1} \alpha_k^p \mathbf{D}_k^{r0} \right) \mathbf{B}_r \quad (15)$$

where \mathbf{D}_k^{r0} is the material property matrix corresponding to the phase material, k -th, including Poisson's ratio ν , and nominal elastic modulus E_k^0 . By using Eq. (13), sensitivities of multi-material stiffness formulation in terms of density variables can be written as follows

$$\frac{\partial \mathbf{K}^e}{\partial \alpha_a^e} = p \alpha_a^{p-1} \sum_{r=\{b,s\}} \int_{\Omega^e} \left[\mathbf{B}_r^T (D_a^{r0} - D_b^{r0}) \mathbf{B}_r \right] d\Omega \quad (16)$$

where α_a^e and \mathbf{U}_e are density of phase 'a' and the element displacement vector of element e -th, respectively. Finally, the sensitivities of objective function C for multi-material topology optimization is written by using the adjoint equation as follows.

$$\frac{\partial C}{\partial \alpha_a^e} = -\mathbf{U}_e^T \frac{\partial \mathbf{K}^e}{\partial \alpha_a^e} \mathbf{U}_e \quad (17)$$

3.4 Computational procedures of multi-material topology optimization of Reissner-Mindlin plates using MITC4

A briefly summarized computational procedures of the present multi-material topology optimization is shown in Fig. 3. This procedure describes optimality criteria-based alternating active-phase algorithm using Gauss-Seidel iteration version of multi-material.

In addition, the multi-material topology optimization for a thick plate structure by using Reissner–Mindlin plate theory is considered. To perform the finite element analysis step, the geometry, material properties, and loading and boundary conditions are determined. By using MITC4 scheme, the shear part of the stiffness matrix is derived from Eqs. (7)-(11). And then the stiffness matrix \mathbf{K} can be calculated by Eq. (15). By linear static analysis $\mathbf{K}\mathbf{U} = \mathbf{F}$, the displacement can be obtained. By using Eq. (16), the sensitivity analysis of objective with respect to element design variables is calculated, and the sensitivity filtering is applied. For the next step, the design variables of a binary sub-problem are updated, and the iterative process continues until the desired optimum convergence, such as the reach of the minimum of compliance or the given number of iterations.

4. Numerical application and discussion

An accurate modeling test of the non-dimensional central displacement of a square plate for several meshes is executed under uniform transverse pressure considering

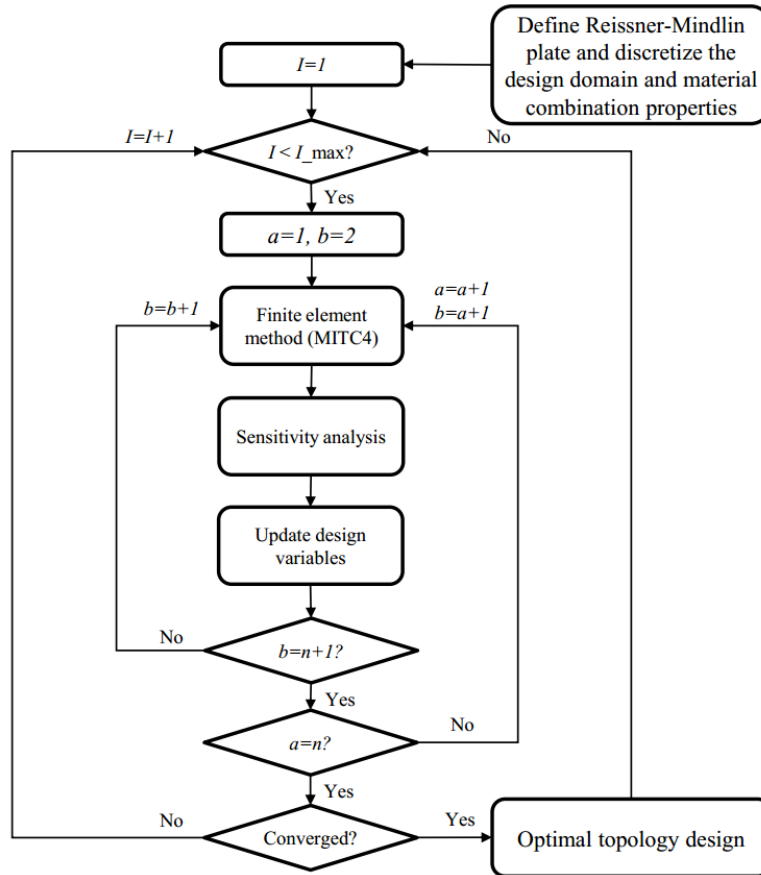


Fig. 3 Flowchart of multi-material topology optimization procedure for thick plates using alternating active-phase algorithm and MITC4

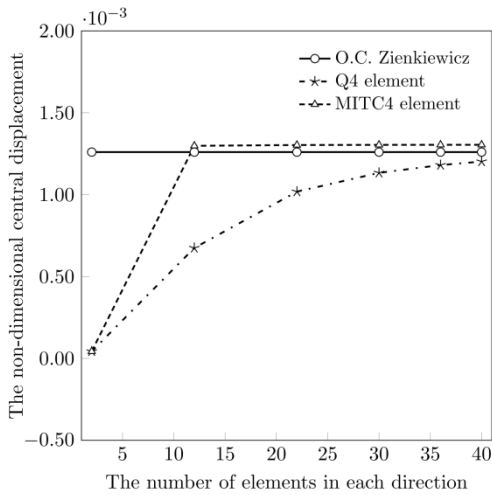


Fig. 4 Accurate modeling test results of fully clamped plate

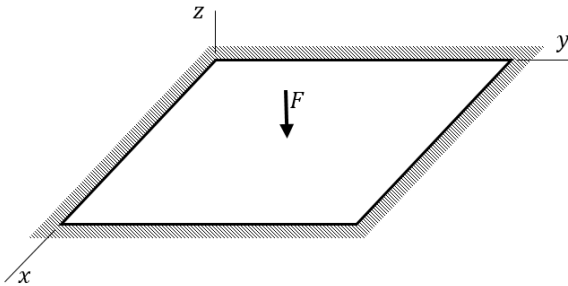


Fig. 5 Definition of load and boundary conditions for steel plate

fully clamped boundary conditions at four sides is shown in Fig. 4. The non-dimensional transverse displacement is set as $\bar{w} = wEt^3 / (23Pl^4(1 - \nu^2))$. Through the increase of element numbers, the present plate model with MITC4 element gradually converges to analytical solutions of Zienkiewicz and Taylor (2000). As can be seen, convergence of MITC4 usage is better than that of Q4 element.

Next, examples of thickness plate structures subject to bending load are carried out as shown in Fig. 5. The structure is modeled as a full y clamped square steel plate. The dimension of the structure is 30×30 and the plate's thickness is constant to be a nominal value of 3. The magnitude of force F is 200. 40×40 MITC4 elements are discretized in a given design domain. The penalization factor for interpolating elasticity properties of stiffness is equal to 3 for all materials. The optimized results are surveyed in cases one, two, three and four various materials. Their material properties are non-dimensional nominal values as shown in Table 1. The material is assumed to be isotropic. Poisson's ratio for all materials is 0.3, which is steel material (Lee 2016). The total volume fraction is fixed to be 40% during every optimization iteration.

Figs. 6, 7, 8 and 9 show optimal topologies of steel thick plates in terms of the assignment of single and multiple materials. As can be seen, optimal topologies of Reissner-Mindlin plates absolutely depend on the number of material types. Multi-material usage may result in the stiffest

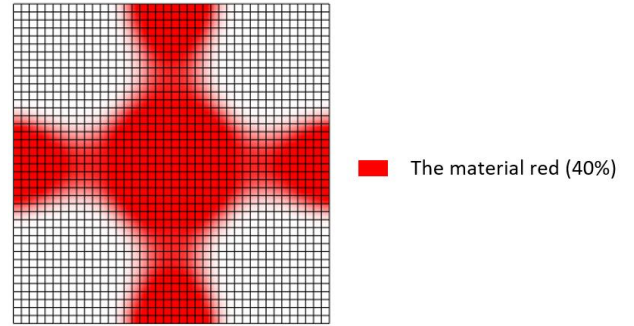


Fig. 6 Optimal Mindlin plate topology with single material ($C = 0.9918$)

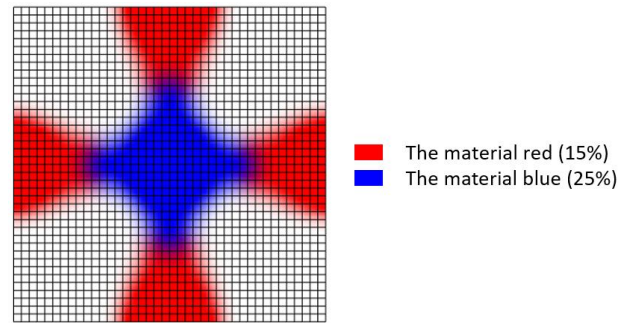


Fig. 7 Optimal Mindlin plate topology with two materials ($C = 0.7791$)

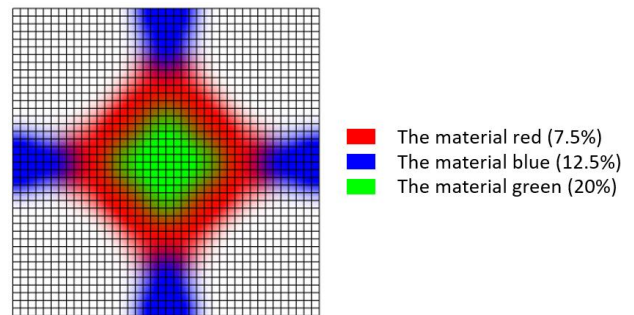


Fig. 8 Optimal Mindlin plate topology with three materials ($C = 0.6797$)

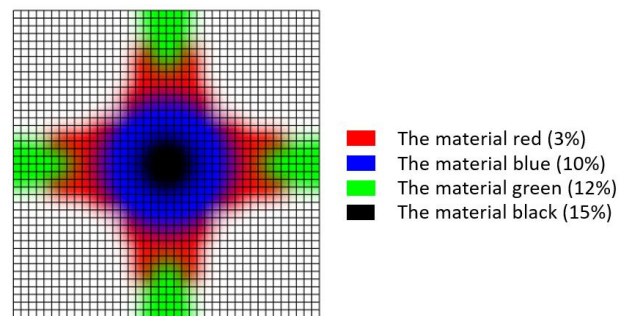


Fig. 9 Optimal Mindlin plate topology with four materials ($C = 0.6001$)

optimal topologies, i.e., the minimal strain energy structures.

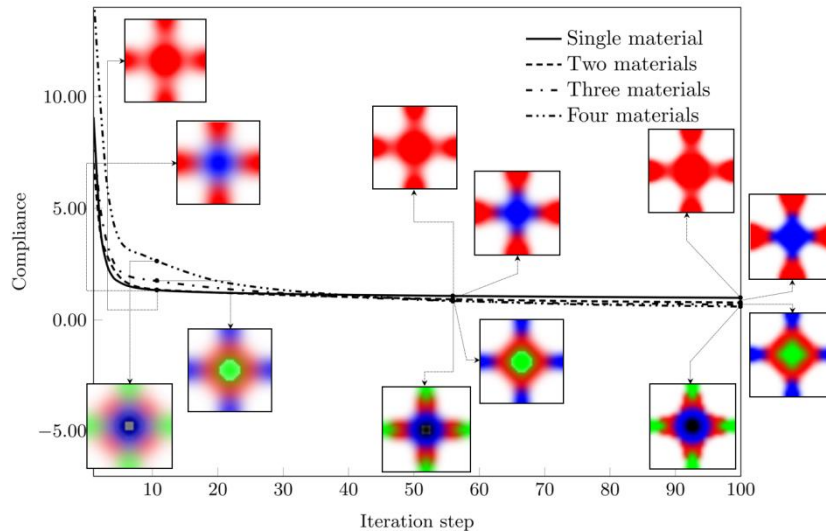


Fig. 10 Convergence histories and optimal intermediate topologies of objective function

Especially, stiff materials are automatically assigned within strong stress concentration regions such as loading points and clamped boundary areas. In this example, applied loading areas have more influence on stiff material assignment than that of clamped boundary areas. Fig. 10 describes convergence histories of objective function (compliance) and intermediate topologies at several iterations. Under the condition of the same amount of total material, multi-material can produce stiffer structure than single material.

5. Conclusions

This study contributes a novel usage of multiple materials for topology optimization of steel plate-like-structures based on Reissner-Mindlin plate theory with MITC4 to avoid shear locking. Numerical applications are conducted to investigate optimal topologies of Reissner-Mindlin plates depending on multi-material types. It would provide design possibilities that multi-material structures using additional stiff materials may produce higher stiffness and offer more cost savings than single material structures, especially in case steel thick plate of this study.

Acknowledgments

This research was supported by a grant (2017R1A2B4001960) from the National Research Foundation of Korea (NRF) funded by the Korea government.

References

- Alonso, C., Ansola, R. and Querin, O.M. (2014), "Topology synthesis of multi-material compliant mechanisms with a sequential element rejection and admission method", *Finite Elem. Anal. Des.*, **85**, 11-19.
- Andreassen, E., Clausen, A., Schevenels, M., Lazarov, B.S. and Sigmund, O. (2011), "Efficient topology optimization in MATLAB using 88 lines of code", *Struct. Multidiscipl. Optimiz.*, **43**(1), 1-16.
- Arnold, D.N., Madureira, A.L. and Zhang, S. (2002), "On the range of applicability of the Reissner-Mindlin and Kirchhoff-Love plate bending models", *J. Elast. Phys. Sci. Solids*, **67**(3), 171-185.
- Banh, T.T. and Lee, D.K. (2018), "Multi-material topology optimization design for continuum structures with crack patterns", *Compos. Struct.*, **186**, 193-209.
- Bathe, K.J. and Dvorkin, E.N. (1985), "A four-node plate bending element based on Mindlin/Reissner plate theory and a mixed interpolation", *Int. J. Numer. Methods Eng.*, **21**(2), 367-383.
- Belblidiaa, F., Leea, J.E.B., Rechakb, S. and Hinton, E. (2001), "Topology optimization of plate structures using a single- or three-layered artificial material model", *Adv. Eng. Software*, **32**(2), 159-168.
- Bendsoe, M. and Kikuchi, N. (1988), "Generating optimal topologies in structural design using a homogenization method", *Computat. Methods Appl. Math.*, **71**(2), 197-224.
- Doan, Q.H. and Lee, D.K. (2017), "Optimum topology design of multi-material structures with non-spurious buckling constraints", *Adv. Eng. Software*, **114**, 110-120.
- Goo, S.Y., Wang, S.Y., Hyun, J.Y. and Jung, J.S. (2016), "Topology optimization of thin plate structures with bending stress constraints", *Comput. Struct.*, **175**, 134-143.
- Lee, D.K. (2016), "Additive 2D and 3D performance ratio analysis for steel outrigger alternative design", *Steel Compos. Struct.*, **20**(5), 1133-1153.
- Lee, D.K. and Shin, S.M. (2015a), "Optimizing structural topology patterns using regularization of Heaviside function", *Struct. Eng. Mech., Int. J.*, **55**(6), 1157-1176.
- Lee, D.K. and Shin, S.M. (2015b), "Automatic position information of web-openings of building using minimized strain energy topology optimization", *Adv. Mater. Sci. Eng.*, 624762.
- Lee, D.K., Yang, C.J. and Starossek, U. (2012), "Topology design of optimizing material arrangements of beam-to-column connection frames with maximal stiffness", *Scientia Iranica*, **19**(4), 1025-1032.
- Lee, D.K., Kim, Y.W., Shin, S.M. and Lee, J.H. (2016), "Real-time response assessment in steel frame remodeling using position-adjustment drift-curve formulations", *Automat. Constr.*, **62**, 57-67.
- Sigmund, O. and Torquato, S. (1997), "Design of materials with extreme thermal expansion using a three-phase topology optimization method", *J. Mech. Phys. Solids*, **45**(6), 1037-1066.

- Tavakoli, R. and Mohseni, S. (2014), "Alternating active-phase algorithm for multimaterial topology optimization problems: a 115-line matlab implementation", *Struct. Multidiscipl. Optimiz.*, **49**(4), 621-642.
- Xia, L., Da, D. and Yvonnet, J. (2018), "Topology optimization for maximizing the fracture resistance of quasi-brittle composites", *Comput. Methods Appl. Mech. Eng.*, **332**, 234-254.
- Yan, K., Cheng, G. and Wang, B.P. (2016), "Topology optimization of plate structures subject to initial excitations for minimum dynamic performance index", *Struct. Multidiscipl. Optimiz.*, **53**(3), 623-633.
- Yun, K.S. and Youn, S.K. (2017), "Multi-material topology optimization of viscoelastically damped structures under time-dependent loading", *Finite Elem. Anal. Des.*, **123**, 9-18.
- Zhou, S. and Wang, M. (2006), "Multimaterial structural topology optimization with a generalized Cahn-Hilliard model of multiphase transition", *Struct. Multidiscipl. Optimiz.*, **33**(2), 89-111.
- Zienkiewicz, O.C. and Taylor, R.L. (2000), *The Finite Element Method: Solid and Fluid Mechanics*, (5th Edition), Volume 2.

CC